Study of Selective Surface of Solar Heat Receiver

Fuad Mammadov

Azerbaijan State Oil Academy, Azerbaijan Republic, AZ1010, Baku city, D.Aliyeva 227

Abstract   For increasing of solar heating energy plants' absorbing possibility and reducing heat loss selective nano-covered surface application has great practical importance. In the investigation $Cu+Ni+SiO_2+Ni+SiO_2$ and $Cu+Ni+ZnS$ content selective nano-covered surface' usage in solar energy plants was studied. This content having high effectiveness was painted on the surface of the specific solar receiver. In comparison with the other selective surfaces this selective nano-covered surface supplies to keep its optical properties stable till T>500℃ temperature. New type solar receiver with the developed selective nano-covered surface was tested in natural condition and at the lab. In the paper the most necessary heat-energy parameters of this solar receiver were defined.

Keywords Solar energy, selective surface, solar receiver, absorption

1. Introduction

For obtaining high effectiveness in solar energy plants solar hear receiver was covered by the special selective layer on the surface. Such surfaces give opportunity to increase maximal effectiveness of solar receiver in sun radiation exchange. Both the cost and the covering technology of the selective layers are too expensive that's why its safety is necessary. Therefore vacuum layer is made around the solar receiver having selective cover, and then it is put into the clear glass pipe. At the expense of vacuum layer selective surface has no relation with the air, convective heat loss reduces to the minimum and the selective layer can be protected from the atmosphere impact for a long time.

At present ray absorption ability of selective cover in solar receivers located in the focus of solar energy plants with high temperature maximally equals 0,94[1]. For effective photo thermal conversion solar receiver surface should have high solar absorption (α) and low heat loss (ε) at the operational temperature. The operational temperature ranges of these materials for solar energy application is divided into low temperature (T<100℃), medium temperature (100℃<T <400℃), and high temperature (T>400℃)[2].

During selective layer covering, clearance class of solar receiver pipe surface should be higher. Thus if the density and smoothness of the selective surface are perfect receiver can work for a long time effectively. While looking on the surface of the existing receivers under the microscope, it is clear that the particles of the selective surface don't form the unite cover.

I can explain this like so, particles of the selective surface

* Corresponding author:
fm_solarpower@yahoo.com (Fuad Mammadov)

can't completely interfere into the nano and micro sized holes on the pipe. Finally surface of the nano sized holes stays beaming and is reflecting sun rays. Besides on the surface of the solar receiver made from the steel material in such holes rust appears, that leads to the rapid destruction of the selective cover[3].

2. Analysis of selective surfaces

Different selective covers (Cu, Ni, SiO, SiO_2, Si_3N_4, TiO_2, Ta_2O_5, Al_2O_3, ZrO_2, Nd_2O_3, MgO, MgF_2, ZnS and SrF_2) are used[4,5] in solar receivers. These layers are covered to the surface on solar receiver in the form of one or more layers. The solar receivers having such selective surfaces are utilized mainly in the parabolic through concentrators. The performance of a candidate solar absorber can be characterized by its solar absorptance and thermal emittance. Using Kirchoff's law, spectral absorptance can be expressed in terms of total reflectance ρ (λ,θ) for opaque materials,

$$\alpha(\lambda,\theta) = 1 - \rho(\lambda,\theta) \qquad (1)$$

and

$$\varepsilon(\lambda,T) = \alpha(\lambda,T) \qquad (2)$$

where $\rho(\lambda,\theta)$ is the sum of both collimated and diffuse reflectance, λ is the wavelength, θ is the incidence angle of light, and T is the given temperature. Development of spectrally selective materials depends on reliable characterization of their optical properties. Using standard spectrophotometers, solar reflectance is usually measured in the 0,3-2,5 μm wavelength range at near-normal $\theta = 0$ angle of incidence. "By experience, this leads to unrealistic predictions of high efficiencies at high temperatures because the emittances are systematically underestimated[6]." Emittance is typically measured at room temperature, though it can be measured at other temperatures. Emittance is frequently reported from reflectance data fitted to blackbody curves

$$\varepsilon = (T) = \frac{\int_{\lambda_{min} \to 0}^{\lambda_{max} \to \infty} [1 - \rho(\lambda,T)] B(\lambda,T) d\lambda}{\sigma T^4} \qquad (3)$$

where $\sigma = 5,6696 \cdot 10^{-8} Wm^{-2}K^{-4}$ is the Stefan-Boltzmann constant and $B(\lambda,T)$ is the spectral irradiance of a blackbody curve from

$$B(\lambda,T) = \frac{c_1}{\lambda^5 \left[e^{\left(\frac{c2}{\lambda T}\right)} - 1 \right]} \qquad (4)$$

where $c_1 = 3,7405 \cdot 10^8 W \mu m^4 m^{-2}$ and $c_2 = 1,43879 \cdot 10^4 \mu mK$ which are Planck's first and second radiation constants, respectively. The actual performance of an absorber at high temperatures may not correspond to the calculated emittance. This is because small errors in measured ρ can lead to large errors in small values of ε[7]. In addition, for some materials the measured emittance data at two different temperatures may simply be different. For example, at λ_{max}, the blackbody wavelength maximum for a specific temperature,
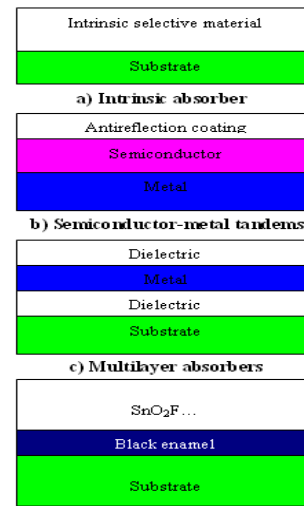
$$\lambda_{max}(\mu) \cdot T(K) = 2898(\mu K) \qquad (5)$$

Emittance is a surface property and depends on the surface condition of the material, including the surface roughness, surface films, and oxide layers[8]. Coatings typically replicate to some degree the surface roughness of the substrate. Therefore to facilitate development, it is important to measure the emittance of each coating-substrate combination as well as the uncoated substrate when developing a solar selective coating. Furthermore, selective coatings can degrade at high temperatures because of thermal load (oxidation), high humidity or water condensation on the absorber surface (hydratization and hydrolysis), atmospheric corrosion (pollution), diffusion processes (interlayer substitution), chemical reactions, and poor interlayer adhesion[9,10]. Calculating the emittance from spectral data taken at room temperature assumes that the spectral characteristics do not change with increasing temperature. This is only valid if the material is invariant and does not undergo a phase change (as do some titanium containing materials), breakdown or undergo oxidation (as do paints and some oxide coatings) at higher temperatures. It is important before using high-temperature emittance calculated from room temperature data, that the calculated data is verified with high-temperature emittance measurements for each selective coating. The key for high-temperature usage is low å, because the thermal radiative losses of the absorbers increase proportionally by the fourth power of temperature; therefore, it is important to measure the emittance at the operating temperatures and conditions[7].

3. Description of Absorber Types

Selective absorber surface coatings can be categorized into six distinct types: a) intrinsic, b) semiconductor-metal tandems, c) multilayer absorbers, and d) selectively solar-transmitting coating on a blackbody-like absorber. In-trinsic absorbers use a material having intrinsic properties that result in the desired spectral selectivity. Semiconductor-metal tandems absorb short wavelength radiation because of the semiconductor bandgap and have low thermal emittance as a result of the metal layer. Multilayer absorbers use multiple reflections between layers to absorb light and can be tailored to be efficient selective absorbers. Additionally, selectively solar-transmitting coatings on a blackbody-like absorber are also used but are typically used in low-temperature applications. These constructions are shown schematically in Figures 1 a-d, respectively, and are discussed in greater detail below.

Figure 1. Schematic designs of four types of coatings and surface treatments for selective absorption of energy

4. The Materials Used

Titanium, zirconium, or hafnium metal carbides, oxides, and nitrides have a high degree of spectral selectivity. The group IV metal compounds are of the general formula MCxOyNz, M=Ti, Zr, or Hf, and x + y + z <2. In these tandem absorber-reflector films, of the compositions studied, substoichiometric compounds of TiNx, ZrNx, and ZrCxNy (on silver) had the best combination of high solar absorptance and low thermal emittance. The absorptance and emittance calculated from reflectance data are summarized in Table 1[11]. TiNx and ZrNx had nearly identical optical properties, but for HfNx the absorptance was lower and the emittance higher. ZrC was the best pure carbide film. Adding carbon to form zirconium carbonitride (ZrCxNy) increased the solar absorptance by 6%. Oxygen, either as suboxides (TiOx and ZrOx) or substituted into the nitrides and carbonitrides (ZrOxNy or ZrCxOyNz) lowered absorptance and raised emittance. A notable exception was an oxidized Zr film with an absorption of 0.93. Solar absorptance was increased by 8% by replacing the aluminum reflective film with an ultrafine dendritic aluminum. Absorptance was also increased by 5% by the addition of number of samples by normal reflectance and total emittance measurements carried out at elevated temperature. Depending on the sample, there

was good agreement with room-temperature measurements up to 400°-600°C. The thermal stability of these tandem absorber-reflector films was studied, and several absorbers survived cumulative heating periods of 500 h in vacuum up to the maximum test temperature, 700°C[12]. The addition of a thin Al_2O_3 diffusion barrier improved the stability in air from 125°C to 175°C[13]. The stability of the tandem films at high temperatures in vacuum was limited to the agglomeration of the metal reflective film, for silver about 350°C. The use of thin layers of Cr_2O_3, Al_2O_3, SiO_2, or other oxide under the metal has been found to stabilize the silver and aluminum and inhibit agglomeration at high temperatures[14]. Agglomeration has been inhibited at temperatures up to 800°C for one hour, but the limit of silver stability achieved was about 500°C[15,16]. The selective optical properties of sputtered ZrC_xN_y on aluminum-coated oxidized stainless-steel are thermally stable from room temperature to 600°C (likely in vacuum but was not specified)[14]. Sputtered selective absorbers with the structure $Al_2O_3/ZrC_xN_y/Ag$ have good optical selectivity with $\alpha/\varepsilon_C(325°C)=0.91/0.05$ at an operating temperature of 700°C in vacuum and 175°C in air[17]. Sputtered $ZrO_x/ZrC_x/Zr$ absorbers have $\alpha/\varepsilon(20°C)=0.90/0.05$ and are thermally stable in vacuum on stainless-steel and quartz substrates up to 600°C and 800°C, respectively[16]. "Raney nickel" type alloys were prepared by co-sputtering nickel, zirconium, or molybdenum with aluminum. After the aluminum was etched out of the $ZrAl_3$ film, a very fine open structure resulted that had a solar absorptance greater than 0.95 and a calculated emittance at 327°C of 0.29[15].

Table 1. Composition and Properties of Selected $MC_xO_yN_z$ absorbers

Antireflective layer	Absorbing layer	Reflective layer	α^1	$\varepsilon(327^0C)^1$
	ZrO_x	Ag	0.72	0.42
	TiO_x	Ag	0.80	0.067
	CrO_x	Ag	0.74	0.079
	ZrN_x	Ag	0.86	0.039
	TiN_x	Ag	0.80	0.034
AlO_x	TiN_x	Ag	0.94	0.170
	HfN_x	Ag	0.76	0.027
	ZrC	Ag	0.81	0.075
	ZrO_xN_y [2]	Ag	0.93	0.071
	ZrC_xN_y	Ag	0.88	0.040
	ZrC_xN_y	Al	0.85	0.074
	ZrC_xN_y	Al [3]	0.93	0.071
AlO_x	ZrC_xN_y	Ag	0.91	0.048
ZrO_x	ZrC_xN_y	Ag	0.64	0.014
	$ZrC_xO_yN_z$	Ag	0.66	0.020
	$ZrAl_3$ [4]	Ag	0.97	0.290

[1] Numerical integration from normal reflectance data, AM2,
[2] Sputtered Zr film "oxidized in hot air,
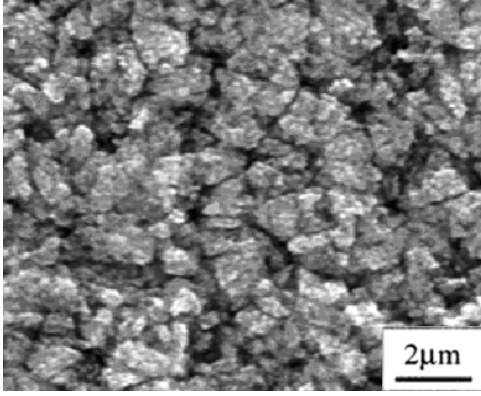[3] Ultra-fine dendritic aluminum,
[4] "Raney"

Methods of combining the characteristics of controlled morphology with intrinsic selectivity deserve further investigation. This work was discontinued in September 1976 and was not resumed. Similar research in Japan appears to have metamorphosed into superconductivity work in 1982[16]. More recent research incorporated the selective properties of pores and created a temperature-stable (400°C), solar-selective coating with a void volume of 22%-26% deposited by reactive evaporation of Ti, Zr, and Hf with nitrogen and oxygen onto copper, molybdenum, or aluminum substrates with a SiO_2 antireflective layer[17]. Solar absorbers could be made by reactive sputtering the nitrides of zirconium, yttrium, cerium, thorium, and europium (i.e., ZrN, YN, CeN, TlN, and EuN), which are transparent in the infrared, abrasion resistant, inert, very hard, and stable at temperatures in excess of 500°C for long periods of time[18]. A recent patent includes ZrN, TiN, HfN, CrN, or $Ti_xAl_{1-x}N$ cermets in an Al_2O_3 dielectric matrix (patent includes TiO_2, ZrO_2, Y_2O_3, SiO_2, Ta_2O_5, WO_3, V_2O_5, Nb_2O_5, and CeO_2) made by the sol-gel technique, where the liquid was applied by spraying or spin coating and heat treated in air at 500°C to 600°C[19]. Additionally, a thin surface film of metal oxynitrides (niobium, tantalum, vanadium, zirconium, titanium, and molybdenum) can be made by coating a substrate with a slurry of a metal halide in a liquid volatile carrier and converting the metal halide to a metal oxide or oxynitride by heating it with oxygen and nitrogen[18]. These materials have some of the highest melting points in nature, with HfC having the highest melting point at 3316°C. The optical properties of these materials have a high degree of flexibility, and with further research, including replacing the stabilized silver with a more thermally stable reflective metal, could be a viable high-temperature absorber for the concentrated solar power program[20].

5. Developement method of Solar Receiver

For parabolic trough concentrator solar receiver was developed which has a new selective nanosurface. Solar receiver consists of cylindric pipe with D/d=132/128 mm diameter and 1400 mm length. Beforehand high smooth surface on the pipe was obtained by the polishing machine. Then in the special oven it stays at 60-80°C temperatures for a while (30-50 sec) for thermal processing and it is cooled. By the specific equipment (SC-400 Precise Coat) the selective layer is covered on the pipe surface in dusting regim. The content of the selective cover consists of $Cu+Ni+SiO_2+Ni+SiO_2$ and Cu+Ni+ZnS, its thickness is 0,013-0,058 nm.

Hereupon, solar receiver is put into the clear glass. Interstice between metal pipe and glass pipe is vacuumized $(P\langle 5\cdot10^{-4}\,mm.mercury\,column)$. On the vacuum layer the high temperature forming on the solar receiver surface can't lose. Maximal limit of the temperature on the receiver surface was 422°C at 1005 W/m² solar radiation.

Figure 2. Scanning Electron Microscope photomicrograph of selective nano surface texture

Figure 3. Dependence of the efficiency on the temperature of solar receiver selective nanocover for different solar radiations (1-200 Wt/m²; 2-400 W/m²; 3-600 W/m²; 4-800 W/m²; 5-1000 W/m²)

In comparison with the simple solar receiver, effective usage quantity of the ideal solar receiver is determined like that:

$$\psi_{ef} = \frac{(\eta_{ptc-reac})}{(\eta_{ptc-reac})_{ideal}} \tag{8}$$

6. Calculation of Concentrator and Solar Receiver System Efficiency

For solar receiver having parabolic trough concentrator and selective nanocover efficiency is calculated like that:

$$\eta_{ptc-reac} = \eta_R \frac{\int\limits_0^\infty \alpha_s(\lambda T_{sns}) \cdot r(\lambda T_s) d\lambda}{\int\limits_0^\infty r(\lambda T_s) d\lambda} -$$

$$-n(\frac{T_{sns}}{T_s})^4 \frac{\int\limits_0^\infty \varepsilon(\lambda T_{sns}) \cdot r(\lambda T_{sns}) d\lambda}{\int\limits_0^\infty r(\lambda T_{sns}) d\lambda} \tag{6}$$
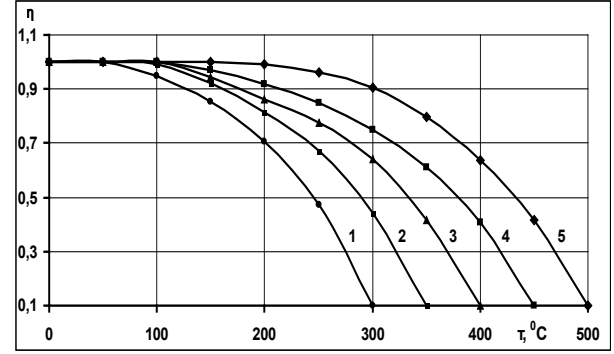
Efficiency of solar receiver having ideal selective nanocover will be so:

$$(\eta_{pk-reac})_{ideal} = \eta_R \frac{\int\limits_0^{\lambda_{opt}} r(\lambda T_s) d\lambda}{\int\limits_0^\infty r(\lambda T_s) d\lambda} -$$

$$-n(\frac{T_{sns}}{T_s})^4 \frac{\int\limits_0^{\lambda_{opt}} r(\lambda T_{sns}) d\lambda}{\int\limits_0^\infty r(\lambda T_{sns}) d\lambda} \tag{7}$$

Here, n - depletion coefficient of sun rays' density on the definite points of the selective nano surface; T_{sns} - temperature of selective nano surface receiving sun rays; T_s - average temperature of solar surface; $r(\lambda T_s)$ - spectral quantity of radiant flux density at T_s temperature of selective nanocover of the solar receiver; $r(\lambda T_{sns})$ spectral quantity of radiant flux density at T_{sns} temperature of selective nanocover of the solar receiver; $\alpha_s(\lambda T_{sns})$ and $\varepsilon(\lambda T_{sns})$ - spectral adsorption-irradiant ability mark of solar receiver selective nanocover.

The efficiency indexes calculated by this method was given at Figure 3.

7. Thermal-Energy Calculation of Solar Receiver

For determining the efficiency of solar receiver having new selective surface heat balance equations are looked through. At stationary regime for solar receiver heat balance equation will be so:

$$q_{ab} = q_{eff} + q_{loss} \tag{9}$$

Here,

$$q_{ab} = K \cdot K_{glass} \cdot A_s \cdot E_g$$

- solar radiation W/m² adsorbed by solar receiver; q_{eff} - effective heat W/m² absorbed by the heat carrier circling in the internal pipe; q_{loss} - the entire heat loss W/m² from the surface of solar receiver; K - concentration coefficient of solar energy; K_{glass} - integral ray transmission coefficient of glass pipe wall; A_s - integral ray absorption of solar receiver; E_g - solar radiation W/m² falling on solar receiver surface.

If heat loss from solar receiver surface equals to the heat loss from the glass pipe surface to the environment, then complete heat loss can be determined:

$$q_{loss} = q_{irr.loss} + q_{con} = q_{irr.glass\blacklozenge} + q_{con.glass} \tag{10}$$

or

$$q_{loss} = \varepsilon_r \varsigma_0 (T_{reac}^4 - T_{glass}^4) +$$

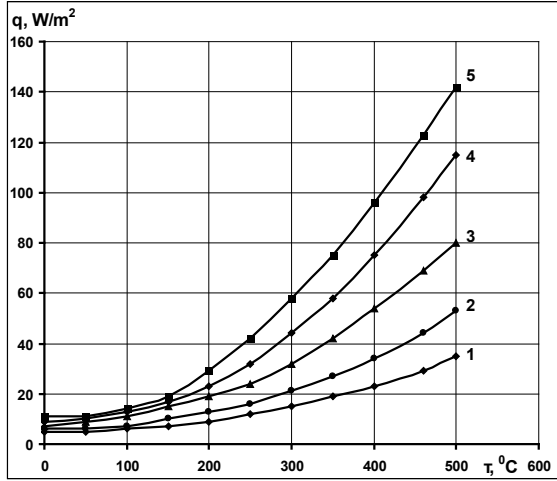$$+ \frac{\lambda_{glass}}{r_{reac} \ln\frac{d_{glass}}{d_r}}(T_{reac} - T_{glass}) = \tag{11}$$

$$= \varepsilon_{glass} \cdot \varsigma_0 (T_{glass}^4 - T_a^4) + \alpha_{glass.a}(T_{glass} - T_a)$$

Here, $q_{irr.loss}$ - heat losses W/m² happened on solar receiver surface by irradiance; q_{con} - possible convective heat loss W/m² between solar receiver and glass pipe; $q_{irr.glass\blacklozenge}$ and

$q_{con.glass}$ irradiation from the glass pipe surface to the environment and heat losses W/m^2 by convection;

$$\varepsilon_{reac} = \cfrac{1}{\cfrac{1}{\varepsilon_r} + \cfrac{d_r}{d_{glass}}\left(\cfrac{1}{\varepsilon_{glass}} - 1\right)}$$

- blackness rate of selective nanocover on the solar receiver. $\varepsilon_{şüş}$ - blackness rate of glass pipe. $\alpha_{glass.a}$ - heat transfer coefficient W/m^2 from glass pipe surface to the environment (air); ς_0 - Stefan-Bolsman constant, W/m^2 K^4; T_{reac}, T_{glass}, T_a - temperatures of glass pipe and air and solar receiver. d_r and d_{glass} - diameter of solar receiver and glass pipe.

Figure 4. Dependence of heat losses from solar receiver surface on temperature for several solar radiations (1-200 W/m^2; 2-400 W/m^2; 3-600 W/m^2; 4-800 W/m^2; 5-1000 W/m^2)

As seen from figure 4 by increasing the temperature on solar receiver surface heat losses become greater. These losses are usually great at high temperatures. The existence of vacuum layer around solar receiver these losses happen by irradiance.

By using equations for heat balance and heat losses of solar receiver thermal efficiency can be determined:

$$\eta_t = \frac{q_{eff}}{KE_g} = \frac{q_{ab} - q_{loss}}{KE_g} \qquad (12)$$

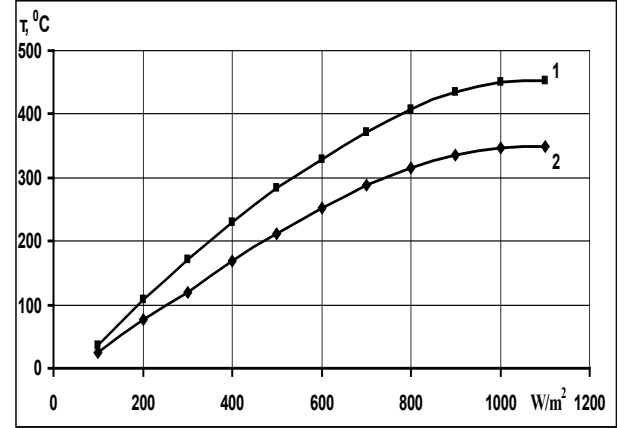Using q_{ab} and q_{loss} for (9) and (11) formulas, the indexes are out in the places:

$$\eta_t = K_{glass}A_s - \frac{1}{kE_g}\left[\begin{array}{l}\varepsilon_r\varsigma_0(T_{reac}^4 - T_{glass}^4) + \\[2mm] + \dfrac{\lambda_{glass}}{r_{reac}\ln\dfrac{d_{glass}}{d_r}}(T_{reac} - T_{glass})\end{array}\right] \quad (13)$$

For (13) using (11) formula:

$$\eta_t = K_{glass}A_s - \frac{1}{kE_g}\left[\begin{array}{l}\varepsilon_{glass}\varsigma_0(T_{glass}^4 - T_a^4) + \\[1mm] + \alpha_{glass.a}(T_{glass} - T_a)\end{array}\right] \quad (14)$$

The calculation of thermal efficiency depends on work regime, work condition, contructive anf optic parameters of solar receiver and glass pipe. Taking into consideration all

these solar receiver effectiveness can be determined.

Figure 5. Dependence of solar receiver selective nanocover temperature on solar radiation (1- by vacuum isolation, 2- by without vacuum isolation)

Table 2. Natural tests results of solar receiver having selective nano-covered surface (July-August, 2011)
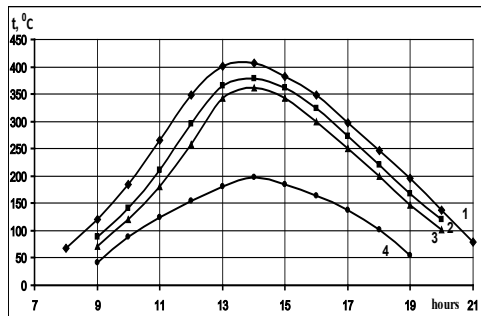
Date	Direct solar radiation, W/m^2	Average air tempera-ture, ℃	Average wind speed, m/sec	selective nano-covered surface tem-perature, ℃	Efficiency %
		July 2011			
1	853	36	2,1	381	0,82
5	879	38	2,8	386	0,84
10	897	38,1	3,5	389	0,84
15	934	39	2,0	392	0,85
20	955	39	1,2	399	0,86
25	968	41	1,1	401	0,87
30	913	40,4	1,5	390	0,85
		August 2011			
1	889	39,6	1,4	388	0,84
5	888	39,5	2,0	388	0,84
10	835	39	1,8	380	0,82
15	802	38,6	2,4	378	0,81
20	754	36	3,3	375	0,79
25	721	35,8	3,8	372	0,79
30	695	33,7	3,5	369	0,77

As seen from figure 5 vacuums isolation influences positive on solar receiver effectiveness. Beginning from marks after 1000 W/m^2 of solar radiation temperature stability appears. At the same condition in the temperature curves on solar receiver surface being studied at the expense of vacuum isolation 105℃ (1100 W/m^2) temperature difference has happened.

At table 2 the experiments; results carried out in 2011, on July-August months have been given. Here on each month in different days direct solar radiation, average air temperature, average wind speed and temperature of selective nanocover on solar receiver surface were measured and noticed. Due to the obtained results efficiency of solar receiver was calculated.

At figure 6 acccording to the natural climatic condition of Absheron peninsula dependence of average temperature of

selective nanocover on day hours was given during the experiments realized on seasons.

Figure 6. Dependence of solar receiver selective nanocover temperature change on day hours due to the seasons. Here on the seasons 1- summer, 2-autumn, 3-spring, 4- winter curves were given

As seen from the figure selective nanocover temperature begining from the morning hours of the day increases till the day time. At 14^{00} reaches to peak rate, then the temperature gradually decreases. These curves on each season during 91/70-80 days have been determined by the experiment.

8. Discussion

The technical parameters of the new selective nanocover:
● High absorption of solar thermal energy α - 96>98% typical 94%
● Low emittance of infra-red radiation ε = 4>10% typical 7%
● Coefficient of thermal expansion 12.5 x 10^{-6} C
These conclusions show that the developed solar receiver having selective nanocover has high effectiveness. So, ray absorption ability is high, heat losses are scanty.

9. Conclusions

While summarizing the final conclusion such decision was obtained that the developed solar receiver having selective nanocover can be used at the following energy plants absorbers:
● Flat plate solar collectors for both hot water and hot air type.
● Parabolic trough and parabolic type collectors.
● Vacuum tube type collectors.
● Passive heating systems.
● A 'Black' body requiring low infra-red emittance.

REFERENCES

[1] J.A. Duffie, W.A. Beckman. Solar Energy Thermal Process. Wiley, New York. 2006, p.928.

[2] Mammadov F.F. Solar energy application for purification and treatment of oily waste in oil fields / Tenth World Renewable Energy Congress and Exhibition 2008, 19-25 July, Glasgow, Scotland. pp. 452-455.

[3] F.F. Mammadov. Use of solar energy in Azerbaijan and modern solar energy plants, Progress, Baku, 2011, p.204.

[4] R. B. Pettit, C. J. Brinker, and C. S. Ashley, "Sol-gel double-layer antireflection coatings for silicon solar cells," Solar Cells, 15, 267 (1985).

[5] A. F. Pereev and N. P. Frolova, "Antireflecting coatings for light-absorbing materials for the 0.4-5 μm spectral region," Sov. J. Opt. Technol., 41, 8, 453 (1974).

[6] C. Seiffert, T. Eisenhammer, M. Lazarov, R. Sizmann, and R. Blessing, "Test facility for solar selective materials," ISES Solar World Congress, 2, 321 (1993).

[7] A. Brunotte, M. Lazarov, and R. Sizmann, "Calorimetric measurements of the total hemispherical emittance of selective surfaces at high temperatures," A. Hugot-Le Goff, C. G. Granqvist, C. M. Lampert, eds., SPIE, 1727, 149 (1992).

[8] R. B. Pettit, "Total hemispherical emittance measurement apparatus for solar selective coatings," SAND-75-0079, Albuquerque, NM: Sandia National Laboratory, 1975.

[9] S. Brunold, U. Frei, B. Carlsson, K. Möller, and,M. Köhl, "Accelerated life testing of solar absorber coatings: testing procedure and results," Solar Energy, 68, 4, 313 (2000).

[10] W. S. Duff and L. Hamasaki, "Experimental evaluation of selective surfaces evacuated solar collectors," R. Campbell-Howe, T. Cortez, and B. Wilkins-Crowder, eds., Proceedings of American Solar Energy Conference, (American Solar Energy Society, Boulder, CO, 1998) p.345.

[11] R. Blickensderfer, "Metal oxycabonitride solar absorbers," Proc. DOE/DS7 Thermal Power Systems Workshop on Selective absorber coatings, P. Call, ed,. SERI TP-31-061, Golden, CO: Solar Energy Research Institute, 1977, p. 371; R. Blickensderfer, D. K. Deardorff, and R. L. Lincoln, "Spectral reflectance of TiN_x and ZrN_x films as selective solar absorbers," Solar Energy, 19, 429 (1977); R. Blickensderfer, U.S. Patent No. 4,098,956, 4 July 1978.

[12] K. D. Masterson and B. O Seraphin, "Investigation of high temperature performance of thin film, solar-thermal energy converters," Arizona Univ. Optical Science Center, Tuscon, AZ, (1976).

[13] D. M. Mattox and R. R. Sowell, "A survey of selective solar absorbers and their limitations," Journal de Physique, C1, n1, 42, (1981).

[14] H. Ihara, S. Ebiswa, and A. Itoh, "Solar-selective surface of zirconium carbide film," Proc. 7th Int. Vac. Cong. and 3rd Int. Conf. on Solid Surfaces, R. Dobrozensky, F. Ruderman, F. P. Viehbock, and A. Breth, eds., (1977) p. 1813.

[15] Y. Noguchi, K. Naka, A. Isao, K. Nakumura, S. Sawada, T. Tani, and S. Gonda, "Fabrication of $ZrCx/Zr$ and $Cr-CrOx$ films for practical solar selective absorption systems," SPIE, 324, 124 (1982).

[16] M. P. Lazarov and I. V. Mayer, U.S. Patent No. 5,670,248, 23 September 1997; M. P. Lazarov and I.V. Mayer, U S. Patent No. 5,776,556, 7 July 1998.

[17] A. H. Lettington and C. Smith, U.S. Patent No. 5,723,207, 3 March 1998.

[18] 197.C. Z. Deng, K. C. Tsai, and D. Ghantous, U.S. Patent No. 5,980, 977, 9 November 1999.

[19] J. A. Thornton and J. A. Lamb, "Evaluation of cermet selec-

tive absorber coatings deposited by vacuum sputtering," SERI Final Subcontract Report SERI/STR-255-3040, Golden, CO: Solar Energy Research Institute, March 1987.

[20] C.E. Kennedy Review of Mid- to High-Temperature Solar Selective Absorber Materials Technical report July 2002, p 58.